Calculation of Bit-Error Probability for a Lightwave System with Optical Amplifiers and Post-Detection Gaussian Noise

Dietrich Marcuse, *Fellow, IEEE*

***Abstract*—This paper is an extension of the analysis presented in a previous paper [1] which dealt with the bit-error probability of a lightwave communication system whose noise contribution was exclusively attributed to spontaneous emission noise of optical amplifiers. In addition, the earlier theory was based on a nonreturn to zero (NRZ) modulation format with zero signal power assigned to logical ZEROES. The present paper extends the earlier theory in several ways. Now, the optical pulses can be much shorter than the bit period (solitons), the power level of logical ZEROES need not vanish, and the thermal noise of the post-detection electronic circuit is taken into account.**

I. Introduction

In an earlier paper [1] we outlined the derivation of the bit-error probability for a lightwave communication system including optical amplifiers whose spontaneous emission was the only source of noise in the system. In addition, we assumed that logical ONES filled their time slot of length T completely and that there was no signal present in the time slot of a logical ZERO.

The present paper is an extension of the earlier paper based on the same mathematical technique but including Gaussian noise originating after the optical signal has been converted to an electrical current. This noise could be thermal noise, shot noise, or a combination of both. Next, we no longer assume that the pulse representing a logical ONE fills its time slot completely. The signal may be much shorter than T, as it would be, for example, in the case of soliton transmission. Finally, logical ZEROES need not be represented by the absence of a pulse but may simply be weaker than pulses representing logical ONES. The shape and duration of the pulses do not affect the bit-error rate since only time averages over one bit interval enter the final results.

As in [1], we express the amplified spontaneous emission noise as a Fourier series that extends only over the interval T of one bit. The signal pulse is represented in the same way. This mathematical device has the advantage that the sine and cosine functions used for series expansions of signal and noise are orthogonal over one bit period, simplifying the analysis of the "integrate and dump" receiver which consists in temporal integration of the signal and noise over the bit interval T. "Integrate and dump" is a special kind of filter which, in many ways, is analogous to an electrical low-pass filter with a bandwidth, $B_{eL} = 1/(2T)$. A discussion of the approximation involved in expressing the time functions as Fourier series expansions over one bit interval is given in the Appendix.

Manuscript received November 20, 1990.

The author is with AT&T Bell Laboratories, Crawford Hill Laboratory, Holmdel, NJ 07733.

IEEE Log Number 9042448.

II. Derivation of the Characteristic Function

We describe the optical electrical signal as a time function $E_s(t)$ and the amplified spontaneous emission noise as a corresponding function $e_{sp}(t)$. These functions are to be understood as the real quantities that are present at the input to the photodetector, such that the short-time averages (indicated by overbars) of their squares are proportional to the corresponding optical powers

$$P_{Ls} = Q\bar{E}_s^2 \tag{1}$$

and

$$P_{Lsp} = Q\bar{e}_{sp}^2. \tag{2}$$

They are also proportional to the photocurrents at the output of the detector

$$I_s = \eta \frac{q}{hf} P_{Ls} = K\bar{E}_s^2 \tag{3}$$

and

$$I_{sp} = \eta \frac{q}{hf} P_{Lsp} = K\bar{e}_{sp}^2. \tag{4}$$

In these equations, η is the quantum efficiency of the detector, h is Planck's constant, q is the magnitude of the charge of the electron, and f is the carrier frequency of the pulses. The connection between the constant Q in (1) and (2) and the constant k appearing in (3) and (4) is

$$K = \eta \frac{q}{hf} Q. \tag{5}$$

A schematic diagram of the lightwave communication system envisioned for the purpose of this study is shown in Fig. 1. The analysis of the bit-error probability simplifies considerably if we expand the signal and amplified spontaneous emission noise, appearing at the input to the photodetector, in Fourier series over the bit-time interval T

$$E_s(t) = \sum_{\nu=-\infty}^{\infty} \mathcal{E}_\nu e^{i\omega_\nu t} \tag{6}$$

and

$$e_{sp}(t) = \sum_{\nu=-\infty}^{\infty} c_\nu e^{i\omega_\nu t} \tag{7}$$

with

$$\omega_\nu = \frac{2\pi}{T}\nu. \tag{8}$$

0733-8724/91/0400-0505$01.00 © 1991 IEEE

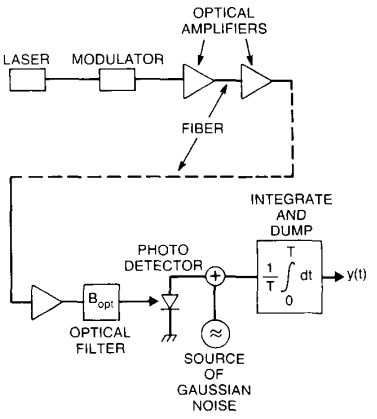

Fig. 1. Schematic of a lightwave system with optical amplifiers.

According to the schematic in Fig. 1, the light passes through an optical filter of bandwidth B_{opt} prior to entering the photodetector. This filter may be either a real optical device placed at the end of the transmission system or it may be a virtual filter representing the band limiting influence of all the amplifiers present in the lightwave system. For the purpose of this analysis the filter is modeled as an ideal bandpass whose transfer function has unit magnitude inside the passband (its phase drops out of the analysis) and is zero outside of it. In the Fourier series representation, the filter covers the range from $\nu = \nu_1$ to $\nu = \nu_2$ with

$$M = \nu_2 - \nu_1 + 1 = B_{\text{opt}} \cdot T. \tag{9}$$

Since $E_s(t)$ and $e_{sp}(t)$ are assumed to the real quantities, the corresponding filtered functions (indicated by a carat) can be expressed as

$$\hat{E}_s(t) = 2 \sum_{\nu=\nu_1}^{\nu_2} \bar{\mathcal{E}}_\nu \cos(\omega_\nu t + \psi_\nu) \tag{10}$$

and

$$\hat{e}_{sp}(t) = 2 \sum_{\nu=\nu_1}^{\nu_2} \bar{c}_\nu \cos(\omega_\nu t + \varphi_\nu) \tag{11}$$

with the definitions

$$\mathcal{E}_\nu = \bar{\mathcal{E}}_\nu e^{i\psi_\nu} \tag{12}$$

and

$$c_\nu = \bar{c}_\nu e^{i\varphi_\nu} = c_{r\nu} + ic_{i\nu} \tag{13}$$

and with

$$\psi_{-\nu} = -\psi_\nu \quad \text{and} \quad \varphi_{-\omega} = -\varphi_\nu. \tag{14}$$

We substitute (10) into (3) and take the time average over one bit period T with the result

$$I_s = 2K \sum_{\nu=\nu_1}^{\nu_2} \bar{\mathcal{E}}_\nu^2. \tag{15}$$

The corresponding time average of the amplified spontaneous emission noise current (4) is

$$I_{sp} = 2K \sum_{\nu=\nu_1}^{\nu_2} \bar{c}_\nu^2 = 2K \sum_{\nu=\nu_1}^{\nu_2} (c_{r\nu}^2 + c_{i\nu}^2). \tag{16}$$

However, since the spontaneous emission noise represents a broad spectrum of random noise we may assume that, on average, the squares of the real and imaginary parts of the expansion coefficients c_ν are identical and are, furthermore, independent of the label ν in the interval $\nu_1 < \nu < \nu_2$

$$\langle c_{r\nu}^2 \rangle \approx \langle c_{i\nu}^2 \rangle = \sigma_c^2 \tag{17}$$

with σ_c^2 indicating the variance of the real and imaginary parts of c_ν. We are thus permitted to write (16) as

$$I_{sp} = 4KM\sigma_c^2. \tag{18}$$

For simplicity, we do not change the notation of I_{sp} even though it is now understood to represent a temporal as well as an ensemble average.

The output of the "integrate and dump" circuit is the random variable

$$y = \frac{K}{T} \int_0^T (\hat{E}_s + \hat{e}_{sp})^2 \, dt + y_{th} \tag{19}$$

with

$$y_{th} = \frac{1}{T} \int_0^T I_{th}(t) \, dt. \tag{20}$$

The constant K in (19) was introduced in (3) and (4) and I_{th} is a current that represents the thermal noise contributions of the electrical circuit and, possibly, shot noise contributed by the photodetector. For our purposes, I_{th} is simply a Gaussian random variable so that its contribution to the output of the "integrate and dump" circuit y_{th} is also a Gaussian random variable [2] with zero mean and with the variance

$$\sigma_{yth}^2 = \langle i_{th}^2 \rangle / T \tag{21}$$

where $\langle i_{th}^2 \rangle$ represents the average of the squared (thermal) noise current per unit bandwidth in units of A^2/Hz.

Substitution of (10) and (11) into (19) yields, with the help of (15)

$$y = I_s + 2K \sum_{\nu=\nu_1}^{\nu_2} \left[c_{r\nu}^2 + c_{i\nu}^2 + 2\bar{\mathcal{E}}_\nu (c_{r\nu} \cos\psi_\nu + c_{i\nu} \sin\psi_\nu) \right] + y_{th}. \tag{22}$$

The probability density $W(y)$ of this function is required to compute the desired bit-error rate. However, it is more convenient to compute the characteristic function, that is the Fourier transform of the probability distribution [2]

$$G_s(\xi) = \int_{-\infty}^{\infty} W_s(y) e^{iy\xi} \, dy. \tag{23}$$

The characteristic function can be regarded as the average of the function $\exp(iy\xi)$. The advantage of using the characteristic function for computing $W(y)$ consists in the fact that, according to the rules of probability theory, the average of $\exp(iy\xi)$ can be computed by using the known (Gaussian) probability distributions of the coefficients $c_{r\nu}$ and $c_{i\nu}$ and the Gaussian probability function of y_{th}. All $c_{r\nu}$ and $c_{i\nu}$ have the same probability distribution which is completely determined by their mean values and their variances σ_c^2. The Gaussian probability distribution of y_{th} is likewise determined by its zero mean and its variance (21). Since the $c_{r\nu}$, $c_{r\nu}$, and y_{th} are all statistically independent, the total probability distribution is the product of

all the individual probability distributions. These considerations permit us to express the characteristic function as follows:

$$G_s(\xi) = \frac{e^{iI_s\xi}}{(2\pi)^{M+1/2}\sigma_c^{2M}\sigma_{yth}} \cdot \prod_{\nu=\nu_1}^{\nu_2} \left\{ \int_{-\infty}^{\infty} \exp\left[\left(-\frac{1}{2\sigma_c^2} + 2iK\xi \right) c_r^2 + 4iK\bar{\mathcal{E}}_\nu \xi c_r \cos\psi_\nu \right] dc_r \right\} \cdot \prod_{\nu=\nu_1}^{\nu_2} \left\{ \int_{-\infty}^{\infty} \exp\left[\left(-\frac{1}{2\sigma_c^2} + 2iK\xi \right) c_i^2 + 4iK\bar{\mathcal{E}}_\nu \xi c_i \sin\psi_\nu \right] dc_i \right\} \cdot \int_{-\infty}^{\infty} \exp\left[-\frac{y_{th}^2}{2\sigma_{yth}^2} + i\xi y_{th} \right] dy_{th}. \quad (24)$$

The integrals in (24) can be found in tables [3]. Using (15) and (18) permits us to write down the following explicit expression for the characteristic function:

$$G_s(\xi) = \frac{\exp\left[-\frac{I_s I_{sp}}{M - iI_{sp}\xi} \xi^2 \right]}{\left(1 - \frac{i}{M} I_{sp}\xi \right)^M} \exp\left(-\frac{1}{2}\sigma_{yth}^2 \xi^2 \right) e^{iI_s\xi}. \quad (25)$$

III. Approximate Solution for the Probability Density

The probability density is obtained as the Fourier inverse of the characteristic function [2]

$$W_s(y) = \frac{1}{2\pi} \int_{-\infty}^{\infty} \frac{\exp\left(-\frac{I_s I_{sp}}{M - iI_{sp}\xi} \xi^2 \right)}{\left(1 - \frac{i}{M} I_{sp}\xi \right)^M} \cdot \exp\left(-\frac{1}{2}\sigma_{yth}^2 \xi^2 \right) e^{i(I_s - y)\xi} \, d\xi. \quad (26)$$

By using the transformation

$$u = 1 - i\frac{I_{sp}}{M}\xi \quad (27)$$

this integral can be written in the form

$$W_s(y) = \frac{M}{2\pi i I_{sp}} \int_{1-i\infty}^{1+i\infty} e^{F(u)} \, du \quad (28)$$

with

$$F_s(u) = \frac{M}{I_{sp}} \left(y - \frac{I_s}{u} \right) (u - 1) - M \ln u + \frac{1}{2} \left(\frac{M}{I_{sp}} \sigma_{yth} \right)^2 (u - 1)^2. \quad (29)$$

An exact solution of this integral seems hard to obtain. However, a very good approximation can be worked out by the well known method of steepest descent [4] which requires us to find the stationary point u_0 of $F(u)$. Thus, we must solve the equation $dF/du = 0$, which can be written in the form

$$u^2 \frac{y}{I_1} - u\frac{I_{sp}}{I_1} - \frac{I_s}{I_1} + M\frac{\sigma_{yth}^2}{I_1 I_{sp}} u^2 (u - 1) = 0. \quad (30)$$

As written, all variables have been expressed as ratios relative to the level I_1 of the average current of a logical ONE. The symbol I_s represents either I_1 itself or the average current of the signal level in a logical ZERO. The ratio of I_1 relative to the average level of the amplified spontaneous emission noise I_{sp} as measured at the input of the photodetector, represents the optical signal-to-noise ratio

$$\text{SNR} = \frac{P_s}{P_{sp}} = \frac{I_1}{I_{sp}}. \quad (31)$$

The third-order equation (30) can be solved exactly. However, computationally it is actually easier to use the iterative Newton method for finding the stationary point $u = u_0$. If the iteration is started with a large value, for example $u = 10$, convergence to the desired result seems assured. Once the stationary point is known, the approximate solution of the integral (28) is [4]

$$W_s(y) = \frac{M}{I_{sp}} \frac{e^{F_s(u_0)}}{\sqrt{2\pi \left(\frac{d^2F_s}{du^2} \right)_{u=u_0}}}. \quad (32)$$

Instead of expressing u_0, $F_s(u_0)$, and $(d^2F_s/du^2)_{u=u_0}$ as functions of the random variable y, it is computationally easier to reverse the situation and express y as well as F_s and its second u-derivative in terms of u_0, so that we have

$$y = I_1 \left[\frac{1}{u_0^2}\frac{I_s}{I_1} + \frac{1}{u_0}\frac{I_{sp}}{I_1} - M\frac{\sigma_{yth}^2}{I_1 I_{sp}} (u_0 - 1) \right] \quad (33)$$

$$F_s(u_0) = M \left[\ln\frac{1}{u_0} + \frac{u_0 - 1}{u_0} - \frac{I_s}{I_{sp}} \frac{(u_0 - 1)^2}{u_0^2} - \frac{M}{2}\frac{\sigma_{yth}^2}{I_{sp}^2} (u_0 - 1)^2 \right] \quad (34)$$

$$\left(\frac{d^2F_s}{du^2} \right)_{u=u_0} = M \left[\frac{2}{u_0^3}\frac{I_s}{I_{sp}} + \frac{1}{u_0^2} + M\frac{\sigma_{yth}^2}{I_{sp}^2} \right]. \quad (35)$$

The steepest descent approximation is very accurate. Its results can be compared with the exact solution of (28) in three special cases. For $\sigma_{yth} = 0$ and $I_s = 0$ the solution is listed in [1]. In this case, the approximation consists in replacing $M!$ by the first term of Stirling's formula [5]. For $\sigma_{yth} = 0$ and $I_s \neq 0$ the exact solution [6] is listed in the Appendix of [1]. Comparison for a number of representative SNR values has demonstrated that the percentage error of the steepest descent approximation is consistently less than 1%. For the special case that all random fluctuations are provided by thermal noise, $I_{sp} = 0$, $I_s \neq 0$, the steepest descent approximation yields the exact Gaussian probability formula.

IV. Bit-Error Rate and Optimal Decision Level

We use the notation $W_1(y)$ to indicate the probability density of the average current y for a logical ONE, that is for $I_s = I_1$. The corresponding probability density for a logical ZERO, $I_s =$

I_0, is designated as $W_0(y)$. The probability for mistaking a logical ONE for a logical ZERO is

$$P_1 = \int_{-\infty}^{y_d} W_1(y)\,dy = \int_{u_{d1}}^{\infty} \left(-\frac{dy}{du_0}\right) W_1(u_0)\,du_0 \quad (36)$$

with y_d indicating the (as yet unknown) optimal decision level of the average detector current y, while $u_{d1} = u_0(y_d)$. The probability for mistaking a logical ZERO for a logical ONE is

$$P_0 = \int_{y_d}^{\infty} W_0(y)\,dy = \int_{0}^{u_{d0}} \left(-\frac{dy}{du_0}\right) W_0(u_0)\,du_0 \quad (37)$$

with $u_{d0} = u_0(y_d)$. The values of u_{d1} and u_{d0} are different from each other and follow from (33) with $I_s = I_1$ or $I_s = I_0$ for a given value of $y = y_d$.

Using (32) through (37), we can express $P_s = P_1$ and $P_s = P_0$ by the following approximation

$$P_s = \sqrt{\frac{M}{2\pi}} \int_{u_{s1}}^{u_{s2}} \sqrt{\frac{2}{u_0^3}\frac{I_s}{I_{sp}} + \frac{1}{u_0^2} + M\frac{\sigma_{yth}^2}{I_{sp}^2}}\, e^{F_s(u_0)}\,du_0 \quad (38)$$

$F_s(u_0)$ is given by (34). The label s assumes the values 0 or 1 in accordance with the association of I_s with the average signal current for a logical ONE or a logical ZERO. The integration limits u_{s1} and u_{s2} depend on the label s in accordance with (36) and (37). We have

$$u_{s1} = u_{d1},\ u_{s2} = \infty; \qquad \text{for } s = 1$$
$$u_{s1} = 0,\ u_{s2} = u_{d0} \qquad \text{for } s = 0. \quad (39)$$

Assuming equal probability, 1/2, for the occurrence of a logical ONE and a logical ZERO, the bit-error rate is

$$\text{BER} = (P_1 + P_0)/2. \quad (40)$$

The optimum decision level is obtained by requiring that BER assumes a minimum value. Since the derivatives of P_1 and P_0 with respect to y are just the probability densities $W_1(y)$ and $W_0(y)$, the optimum decision level $y = y_d$ is obtained as the solution of the equation

$$W_1(y_d) = W_0(y_d). \quad (41)$$

Solving this equation requires that we express W_1 and W_0 by means of (32), using (34) through (35). Next we must search for values of u_{d1} and u_{d0} such that the corresponding $y = y_d$, obtained from (33), satisfies (41).

The integral in (38) can probably not be evaluated exactly. A numerical solution is not hard to compute. However, a satisfactory approximation can be obtained as follows. We write the integral in the form

$$P_s = \sqrt{\frac{M}{2\pi}} \int_{u_{s1}}^{u_{s2}} e^{G_s(u)}\,du \quad (42)$$

with

$$G_s(u) = F_s(u) + \frac{1}{2}\ln\left(\frac{2}{u^3}\frac{I_s}{I_{sp}} + \frac{1}{u_0^2} + M\frac{\sigma_{yth}^2}{I_{sp}^2}\right). \quad (43)$$

Since the probability of finding y near the optimum decision level y_d must be low, the exponential function $\exp[G_s(u)]$ must vary rapidly near $y = y_d$, or near one of the corresponding integration limits, for example, $u = u_{s2}$. In other words, at the integration limit, $u_{s2} = u_{ds}$, the integrand assumes its maximum value and falls very steeply as the integration variable moves away from u_{ds} deeper into the integration range. This means that the principal contribution to the integral comes from the region of the immediate vicinity of $u = u_{ds}$. This permits us to expand

$$G_s(u) = G_s(u_{ds}) + \frac{dG_s}{du}(u - u_{ds}) \quad (44)$$

and to approximate the integral as

$$P_s = \sqrt{\frac{M}{2\pi}} \frac{\exp[G_s(u_{ds})]}{\left|\dfrac{dG_s(u_{ds})}{du}\right|}. \quad (45)$$

Introducing the abbreviations

$$A_s = 2\frac{I_s}{I_{sp}} + u_{ds} + M\frac{\sigma_{yth}^2}{I_{sp}^2}u_{ds}^3 \quad (46)$$

and

$$B_s = 3\frac{I_s}{I_{sp}} + u_{ds} \quad (47)$$

we can express the probability P_s as follows:

$$P_s = \sqrt{\frac{MA_s}{2\pi u_{ds}^3}} \frac{\exp[F_s(u_{ds})]}{\left|\dfrac{u_{ds} - 1}{u_{ds}^3}MA_s + \dfrac{B_s}{u_{ds}A_s}\right|}. \quad (48)$$

In this formula, the label s is either $s = 1$ for the probability of making an error in identifying a logical ONE, or $s = 0$ for an erroneous identification of a logical ZERO. The parameter u_{ds} is the solution of (33) for $y = y_d$ where y_d must be adjusted to be the solution of (41). It is thus clear that the evaluation of the bit-error rate requires a fair amount of numerical computation.

Many of our formulas contain the parameter I_{sp} in the denominator. Thus, when we consider the case of pure thermal noise, $I_{sp} = 0$, it is necessary to evaluate our results as the limit $I_{sp} \to 0$. It is straightforward to show that, in this limit, (32) results in a Gaussian probability distribution with mean value I_s and variance σ_{yth}^2. The optimal decision level is found to be

$$y_d = (I_1 + I_0)/2 \quad (49)$$

and (46) through (48) result in

$$P_s = \frac{1}{\sqrt{2\pi}\,Q} e^{-(1/2)Q^2} \quad (50)$$

with

$$Q = \frac{I_1 - I_0}{2\sigma_{yth}}. \quad (51)$$

These are indeed the results to be expected for random Gaussian noise.

V. Gaussian Approximation

The optical electric field of the spontaneous emission noise has a Gaussian probability distribution. However, after detection the noise contributions to the detected current consist in beats between the signal and the amplified spontaneous emission noise [the terms in c_{rv} and c_{iv} in (22)] and in noise-noise beats [the second-order terms in c_{rv} and c_{iv} in (22)] of the spontaneous emission with itself. Since the signal is not a random variable, the signal-noise beats retain the Gaussian probability distribution. But the noise-noise beats by themselves have a chi-

square distribution which becomes Gaussian only in the limit of $M \to \infty$.

Our analysis of the bit-error rate, including rectified optical spontaneous emission and additive Gaussian noise, shows the complexity of this problem. Thus, it is tempting to ignore the true nature of the statistics and pretend that all random fluctuations of the detector current obey Gaussian statistics. This approach is indeed often followed [7], [8] when only an order-of-magnitude estimate of the bit-error rate is desired. Since the Gaussian statistics is uniquely determined by the mean value and the variance of the time-averaged detected current y, it is sufficient to know these quantities to be able to formulate the bit-error rate in the Gaussian approximation. The mean and variance of y can be obtained from derivatives of the characteristic function (25) without any further approximation [2]. From (25) we obtain

$$\langle y_s \rangle = -i \left(\frac{\partial G_s}{\partial \xi} \right)_{\xi = 0} = I_s + I_{sp} \tag{52}$$

and

$$s_{ys}^2 = \left\langle \left(y - \langle y_s \rangle \right)^2 \right\rangle = -\left(\frac{\partial^2 G_s}{\partial \xi^2} \right)_{\xi = 0} - \langle y_s \rangle^2$$

$$= \frac{1}{M} I_{sp}(2I_s + I_{sp}) + \sigma_{yth}^2. \tag{53}$$

We use the symbol s_{ys} for the variance of y to avoid confusion with the variance of the thermal noise portion of the time-averaged detected current. With these quantities we can write down the Gaussian approximation of the probability density of y

$$W_{gs}(y) = \frac{1}{\sqrt{2\pi} s_{ys}} \exp \left[-\frac{\left(y - \langle y_s \rangle \right)^2}{2 s_{ys}^2} \right]. \tag{54}$$

To determine the optimal decision level, we compare the exponents of W_{g1} and W_{g0} for $y = y_d$ and obtain

$$y_d = \frac{\langle y_1 \rangle s_{y0} + \langle y_0 \rangle s_{y1}}{s_{y0} + s_{y1}}. \tag{55}$$

This value is not quite exact since the variances s_{y1} and s_{y0}, that appear in the denominator of (54), are not identical. However, the exponential function varies so rapidly near $y = y_d$ that only a small error results from our approximation.

Using again the approximation that leads to (45), we obtain from (40) the following formula for the bit-error rate in Gaussian approximation:

$$\text{BER} = \frac{1}{\sqrt{2\pi} Q} e^{-(1/2)Q^2} \tag{56}$$

with

$$Q = \frac{\langle y_1 \rangle - \langle y_0 \rangle}{s_{y0} + s_{y1}}. \tag{57}$$

VI. Numerical Examples

In order to be able to compute numerical values of BER, using (40) and (46) through (48), we need to know several experimental quantities. The most important quantity is the optical signal to (spontaneous emission) noise ratio (31) and the ratio

$$R_{01} = I_0 / I_1 \tag{58}$$

of the average current in a pulse representing a logical ZERO to the average current in a logical ONE. These quantities are used to compute the probabilities P_1 and P_0 from (48) and BER from (40).

So far we have assumed that the spontaneous emission noise is polarized in the same direction as the signal light. For unpolarized noise the number of terms in the Fourier expansion of spontaneous emission noise doubles, since there is now an additional degree of freedom for each spectral component. This doubling of noise components does not affect the Fourier expansion of the signal and it also does not affect the signal-noise beats since the signal beats only with noise in its own polarization state. It is easy to see that in (25) the quantity M appears only in connection with noise-noise beats in the combination I_{sp}/M so that this ratio is actually constant since I_{sp} doubles if an additional noise component with the opposite polarization is added. This means that we must modify (9) to read

$$M = pB_{\text{opt}} \cdot T \tag{59}$$

with $p = 1$ for polarized noise and $p = 2$ for unpolarized noise.

Finally, it is necessary to know what value to insert for the variance of the additive Gaussian noise which is introduced after photodetection. Equation (21) gives a prescription for computing the variance of the Gaussian noise component in terms of the square-averaged current associated with this noise per unit bandwidth and per time interval T. If there is negligible detector shot noise, so that σ_{yth} is totally associated with thermal noise, we may use the Nyquist relation for matched circuits [2]

$$\langle i_{th}^2 \rangle = kT_k / R \tag{60}$$

with $k = 1.38 \times 10^{-23}\ J/K$ and T_k indicating the temperature in degrees Kelvin. R is the impedance of the detector circuit. For our examples we use $R = 50\ \Omega$. Thus, we have from (21)

$$\sigma_{yth}^2 = \frac{kT_k}{RT}. \tag{61}$$

If instead of an "integrate and dump" circuit an electrical low-pass filter of bandwidth B_{eL} is used, we may replace

$$T = 1/(2B_{eL}). \tag{62}$$

Our choice of $R = 50\ \Omega$ for the impedance of the detector circuit is, of course, purely arbitrary and by no means an optimum. Good optical receivers have high-impedance "front ends" which, according to (60), reduce the amount of thermal noise.

If the additive Gaussian noise of the photodetector includes significant amounts of shot noise, the variance (61) would have to be augmented by an additive term to take this into account. Furthermore, we would need a different value of σ_{yth} for logical ONES and logical ZEROES, since the amount of shot noise would depend on the nature of the received signal. For this reason, we would have to attach the index s to the variance of the Gaussian noise and use different values of σ_{yths} for ONES and ZEROES in (46) and (53).

Because of the large number of parameters it is impossible to give comprehensive graphical representations of BER for all interesting cases. In [1] we presented graphs of BER as functions of the normalized signal-to-noise ratio for several values of the product $B_{\text{opt}} \cdot T$. In this paper we want to highlight the influence of additive thermal noise, since it is the most important new feature that has been added to the theory. To do this, we plot the quantities of interest as functions of the average optical sig-

nal power (averaged over the bit period T of a single time slot) measured at the input to the photodetector. The relation between optical power and detector current is given by (3). We use a quantum efficiency of 100%, $\eta = 1$. The bit period is $T = 0.4$ ns (2.5 Gb/s) and the wavelength is $\lambda = 1.55$ μm in all cases. For small optical input powers, thermal noise predominates, while the curves saturate for large input power.

Fig. 2(a)–(d) show the normalized optimum decision level $(y_d - I_0)/(I_1 - I_0)$ as a function of the average optical input power P_{L1} (pulse power in a logical ONE averaged over one time slot) for several values of the optical signal-to-noise ratio. The value of $M = pB_{opt} \cdot T$ is different for each figure but $R_{01} = I_0/I_1 = 0$ applies to all figures. In viewing these figures it should be remembered that the spontaneous emission noise power is decreasing simultaneously with the light power since SNR is kept constant. For the same reason the curves level off for large input power as the amplified spontaneous emission noise overwhelms the thermal noise. For large SNR the normalized decision level approaches 1/2 as the input power to the photodetector approaches zero. For small values of SNR the normalized optimal decision level exceeds 1/2 since, according to (52), the spontaneous emission noise makes a significant contribution to the average signal level which is now significantly higher than I_0 and I_1, so that the decision level is pushed up as well.

Fig. 3(a)–(d) are similar to Fig. 2, except that now the ratio of the average current in a ZERO to the average current in a ONE is $I_0/I_1 = 0.1$. These curves look very similar to those in Fig. 2. The most important difference consists in the fact that the level of the normalized curves in Fig. 3 is somewhat higher than that of the curves in Fig. 2 since we now have significant signal-noise beats also for the ZERO level.

The logarithm of the bit error rate is plotted in Fig. 4(a)–(d) for $I_0/I_1 = 0$ as a function of the optical power at the input to the photodetector. The pulse power is averaged over the time interval of one bit representing logical ONES.

Let us emphasize that it is important to remember that the shape and duration of the pulses does not influence the bit-error rate since only the time average of the pulses, taken over the bit interval T, enters the final result.

The value of $M = pB_{opt} \cdot T$ varies from Fig. 4(a) to (d) from 1 to 50. The solid curves represent the result of the full theory of this paper while the dotted curves represent the Gaussian approximation. We see that the Gaussian approximation overestimates the bit error rate by as much as one order of magnitude (remember that the logarithm is plotted in the figures).

The rise of the bit-error rate curves for small input powers is caused by the thermal noise of the detector circuit. The details of this part of the curves depend in our assumptions of the circuit impedance (50 Ω in our case) and on whether the noise is of thermal origin or is augmented by shot noise of the photodetector, which is not included in our examples. However, as P_{L1} increases, the influence of thermal and shot noise decreases. The asymptotic values for large P_{L1} seen in Fig. 4 (and Fig. 5) represent the limiting case where the noise is completely dominated by amplified spontaneous emission.

At first glance it may appear odd that much smaller values of SNR are required to achieve a given bit-error rate as the value of $M = pB_{opt} \cdot T$ is increasing. To understand this behavior it is important to remember that the amount of spontaneous emission noise arriving at the detector increases linearly with increasing bandwidth of the optical filter so that, for fixed signal power, SNR decreases with increasing values of M. However,

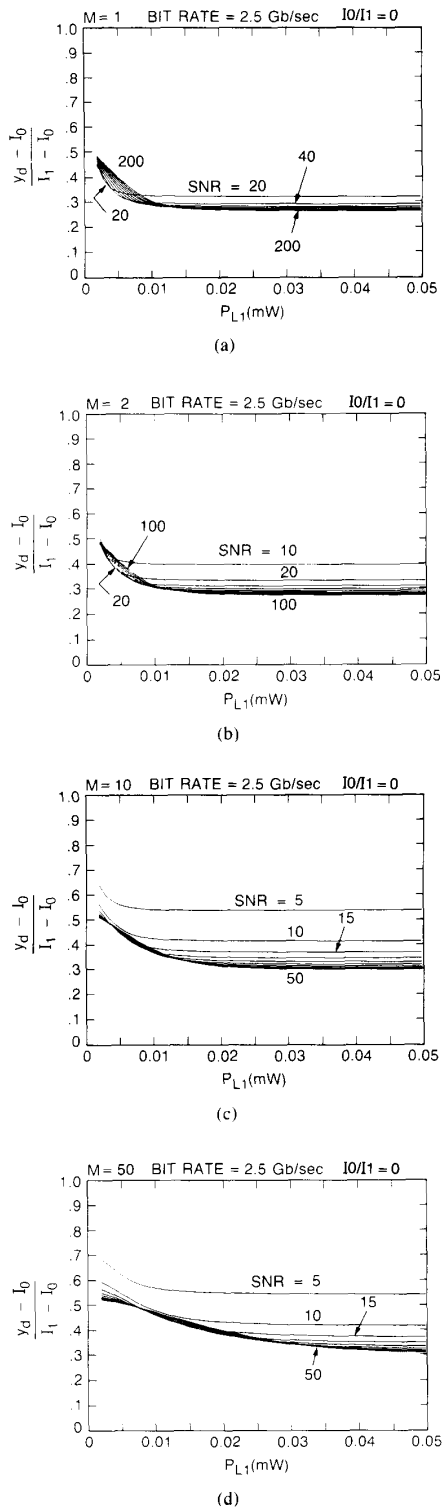

Fig. 2. Normalized optimal decision level as a function of light power in a logical ONE (at the input to the photodetector, averaged over one bit period). The numbers labeling different curves represent the optical signal-to-noise ratio. $I_0/I_1 = 0$ for all curves. (a) $M = 1$. (b) $M = 2$. (c) $M = 10$, and (d) $M = 50$.

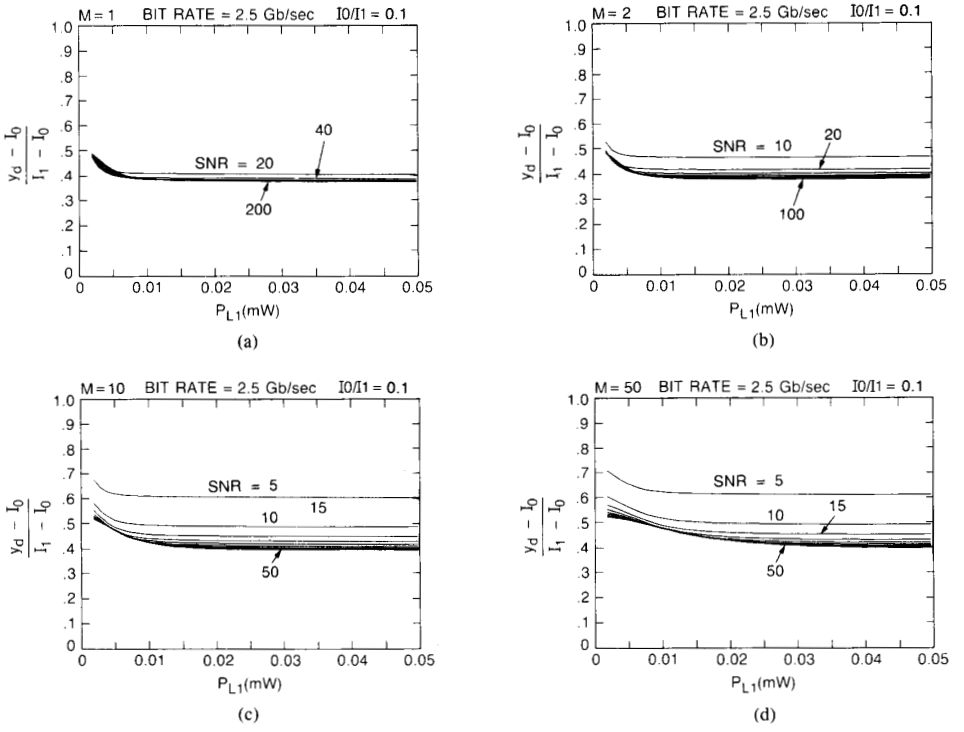

Fig. 3. Similar to the Fig. 2(a) through (d) for $I_0/I_1 = 0.1$.

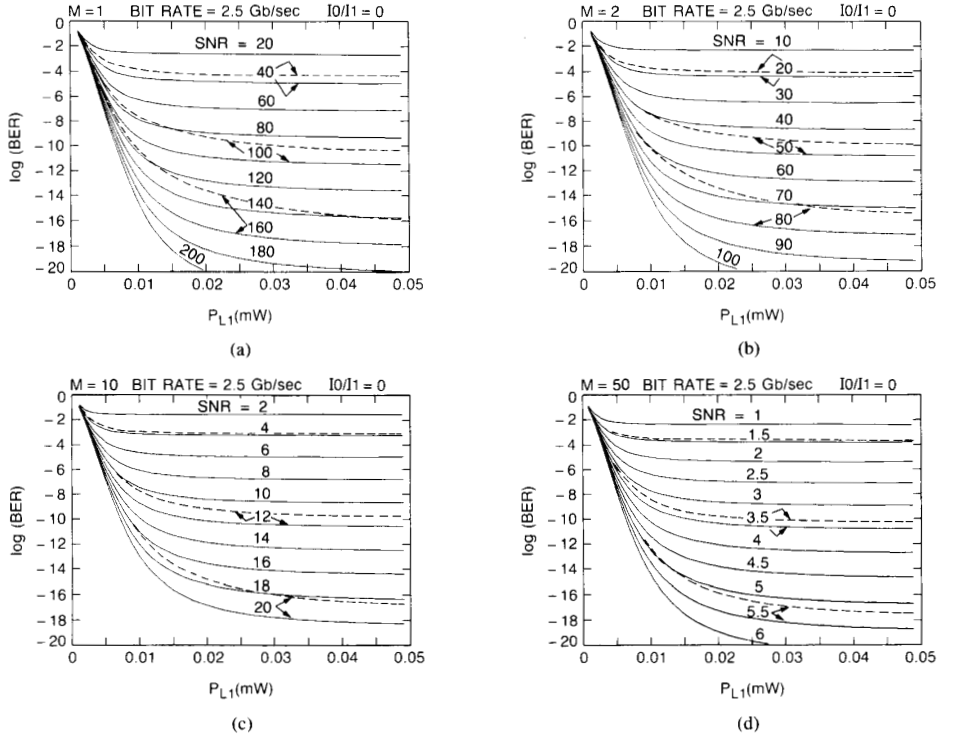

Fig. 4. Logarithm (base 10) of the bit-error rate as a function of optical input power to the photodetector in logical ONES, averaged over one time slot for several values of SNR. The solid curves represent the theory of this paper, the dotted curves display the Gaussian approximation. For all curves $I_0/I_1 = 0$. (a) $M = 1$, (b) $M = 2$, (c) $M = 10$, and (d) $M = 50$.

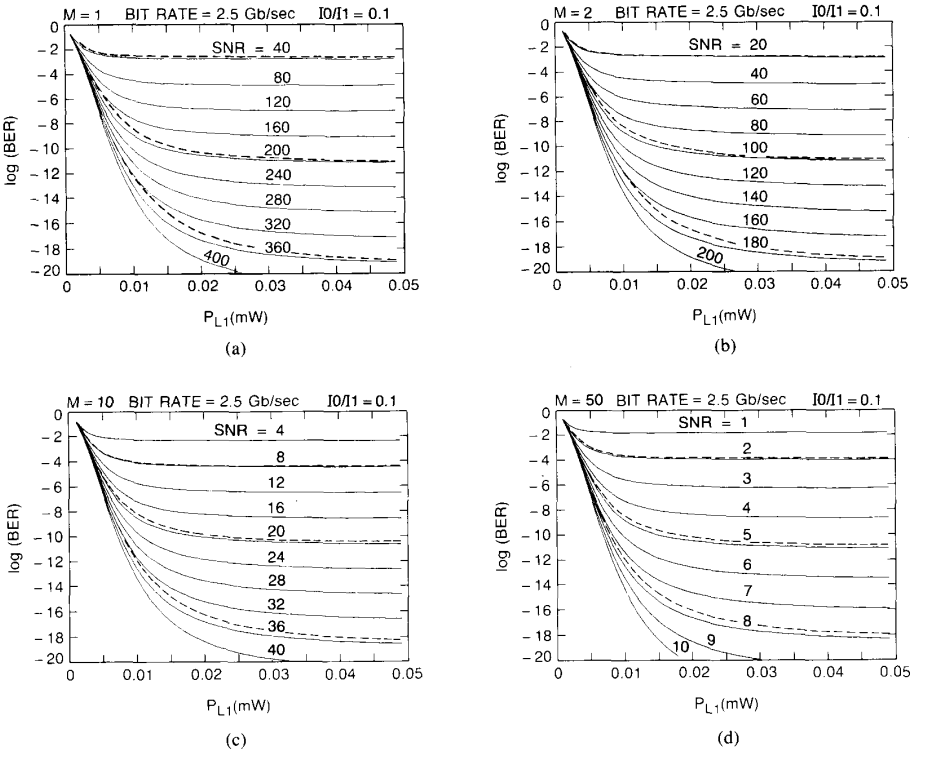

Fig. 5. Similar to Fig. 4(a) through (d) but for $I_0/I_1 = 0.1$.

increasing the filter width does not increase the signal-noise beats, provided all of the frequency components contained in the signal spectrum can pass the optical filter. The signal beats with the noise only with those frequency components that carry signal power. However, with increasing M the noise-noise beats increase so that the BER becomes relatively poorer even though noise-noise beats are not as effective as signal-noise beats in degrading the bit-error rate.

The bit-error rate curves in Fig. 5(a)–(d) are very similar to those of Fig. 4 except that now $I_0/I_1 = 0.1$. There are two important differences between Figs. 4 and 5. If the power level in logical ZEROES does not go down to zero, $I_0 > 0$, a higher signal power is required in the logical ONES to achieve the same bit-error rate. Secondly, the Gaussian approximation is considerably better in this case because signal-noise beats, occurring also at the ZERO level, have Gaussian statistics and carry more weight than noise-noise beats.

VII. Conclusions

We have derived an accurate theory for the bit-error rate of a lightwave system incorporating optical amplifiers so that the system noise is a combination of amplified spontaneous emission and additive thermal (or other Gaussian) noise generated in the electrical detector circuit. The bit-error calculation is based on pulse modulated light signals. However, the pulses need not occupy the entire length of the time slot, their shape and duration is arbitrary, so that the theory applies, among other cases, to soliton transmission. The only quantity of interest is the time-averaged power (averaged over one time slot) appearing at the input of the photodetector. Finally, we permit logical ZEROES to carry nonvanishing light power.

This theory, an extension of earlier work [1], [9], is considerably more complicated due to its greater generality. Its evaluation requires the numerical solution of transcendental equations, but it does not require numerical integrations.

The results of this theory are compared with the much simpler Gaussian approximation. We find that the Gaussian approximation can overestimate the bit-error rate by an order of magnitude if the signal power vanishes for logical ZEROES. The agreement between the Gaussian approximation and the more complex theory becomes better when the pulse power of logical ZEROES does not vanish. However, for given average pulse power in logical ONES this mode of operation results in a higher bit-error rate.

The implications of the theory are illustrated by a number of numerical examples that are plotted in Figs. 4 and 5.

Appendix

In this Appendix we discuss briefly and qualitatively the implication of our practice of expanding the time functions (10) and (11) as Fourier series over the base domain T, where T is equal to the bit interval and also the time interval over which the detected signal is integrated. Inside of this base interval the Fourier series represents the function correctly (disregarding a possible Gibbs phenomenon at the boundaries of the domain). But the Fourier series expansion has the property of forcing the function that it expresses to become periodic with period T, so that the autocorrelation function of a random process also becomes periodic. As long as we are interested in the function only within the preselected bit time interval T, the enforced periodicity outside of this interval poses no problem. For example, if we are dealing with random noise of very large bandwidth

and a correlation time that is much shorter than T, the noise elements in adjacent intervals of length T are statistically independent, so that we are justified in concentrating on a single interval. However, if the noise is filtered prior to detection, the filter enforces correlations on the output signal so that the noise in one time interval depends on the noise in at least the immediately preceding interval. In that case we may not be allowed to concentrate on just one time interval.

This discussion makes it clear that we should be concerned with the correlations existing in filtered random noise. But if the correlation imposed by the filter turns out to be negligible, we may concentrate on a single time interval, disregarding neighboring intervals and expand our function in a Fourier series over just this time interval.

According to (19) the time-averaged detected current contains two random components (disregarding the additive thermal noise term y_{th}). One is the noise-noise beat term, $\hat{e}_{sp} \cdot \hat{e}_{sp}$ (which we shall mention briefly at the end of this discussion), the other is the signal-noise beat term, $\hat{E}_s \cdot \hat{e}_{sp}$. This latter contribution can be analyzed easily, since $\hat{E}_s$ is a deterministic function and only the filtered noise, $\hat{e}_{sp}$, is a random function. We concentrate on the essential part of this random signal and investigate the correlation of

$$y_i = \frac{1}{T}\int_{t_i}^{t_i+T} \hat{e}_{sp}(t)\, dt \tag{A1}$$

obtained in two adjacent time intervals of length T. The y functions in the two adjacent intervals are designated as y_1 and y_2. Since we are concerned with correlations introduced by the optical filter of bandwidth B_{opt}, we must now use a Fourier series expansion over a very large time interval τ which approaches ∞. This analysis consists in substituting the series expansion (11) into (A1), except that T in (8) is now replaced with the much larger time interval τ. We use once more the ideal square-shaped filter that was used throughout this paper. In addition, we assume that the Fourier coefficients at different frequencies are mutually uncorrelated. This latter assumption is correct for unfiltered random noise and is not changed by multiplying the spectral noise components with the transfer function of the filter. A straightforward analysis yields the following expression for the correlation coefficient

$$r = \frac{\langle y_1 y_2 \rangle}{\sqrt{\langle y_1^2 \rangle \langle y_2^2 \rangle}} = \frac{\displaystyle\int_0^{B_{\text{opt}} \cdot T} \frac{1}{x^2} \sin^2(\pi x) \cos(2\pi x)\, dx}{\displaystyle\int_0^{B_{\text{opt}} \cdot T} \frac{1}{x^2} \sin^2(\pi x)\, dx}. \tag{A2}$$

Fig. 6 represents a plot of the correlation coefficient as a function of the product $B_{\text{opt}} \cdot T$ which shows how rapidly the correlation coefficient decreases from unity to small values. In any practical lightwave system we will always have $B_{\text{opt}} \cdot T \geq 1$ so that we can be assured that $r < 0.05$. Thus, there is very little correlation between the time-averaged noise contributions in adjacent time slots which justifies our use of the Fourier expansion over just a single time slot.

I have checked the correlation curve in Fig. 6 with computer simulated experiments and found very good agreement. In addition, the curve did not change significantly when the ideal square filter was replaced with a realistic Butterworth filter of order 4. Finally, I used the computer simulation to compute the correlation coefficient for the time-averaged noise-noise beats

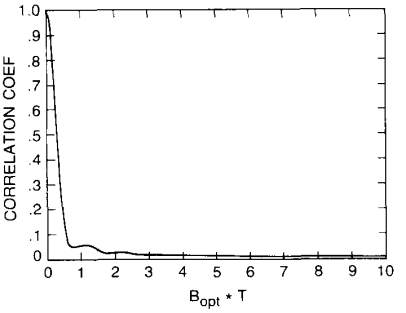

Fig. 6. Correlation coefficient for the average noise in adjacent time slots of length T as a function of $B_{\text{opt}} \cdot T$.

and found that it too decreases rapidly in essentially the same way as the curve in Fig. 6. These studies do not provide a quantitative bound on the error of BER as computed with the analysis presented in this paper, but they help to build confidence in the results presented here. In particular, it should be clear that our results improve with increasing values of $M = pB_{\text{opt}}T$, because of the rapid decrease of the correlation coefficient with increasing values of M.

REFERENCES

[1] D. Marcuse, "Derivation of analytical expressions for the bit-error probability in lightwave systems with optical amplifiers," *J. Lightwave Technol.*, vol. 8, pp. 1816–1823, 1990.
[2] A. Papoulis, *Probability, Random Variables, and Stochastic Processes* 2nd ed. New York: McGraw-Hill, 1984.
[3] I. S. Gradshteyn and I. M. Ryzhik, *Tables of Integrals, Series and Products.* New York: Academic, 1980.
[4] P. M. Morse and H. Feshbach, *Methods of Theoretical Physics Part I.* New York: McGraw-Hill, 1953.
[5] M. Abramowitz and I. A. Stegun, "Handbook of Mathematical Functions," National Bureau of Standards, Applied Mathematics Series 55, 1964.
[6] J. I. Marcum and P. Swerling, "Studies of target detection by pulsed radar," IRE Transact. on Information Theory, IT-6, 59-267, 1960.
[7] R. G. Smith and S. D. Personick, "Receiver design for optical communications systems," in *Topics in Applied Physics, Vol. 39, Semiconductor Devices for Optical Communications, Ed. H. Kressel,* New York: Springer, 1980.
[8] N. A. Olsen, "Lightwave systems with optical amplifiers," *J. Lightwave Technol.*, vol. 7, pp. 1071–1082, 1989.
[9] P. S. Henry, "Error-rate performance of optical amplifiers," *Optical Fiber Commun. Conf. 1989, Tech. Dig. Series*, vol. 5, THK3.

*

Dietrich Marcuse (M'58–F'73) was born in Koenigsberg, East Prussia, Germany, on February 27, 1929. He received the Diplom-Physiker degree from the Freie Universität, Berlin, West Germany, and the Dr.Ing. degree from Technische Hochschule, Karlsruhe, West Germany, in 1954 and 1962, respectively.

From 1954 to 1957 he worked at the Central Laboratory, Siemens and Halske, Berlin, West Germany, on transmission-line problems and the development of the circular waveguide. In 1957 he became a Member of the Technical Staff at Bell Laboratories, Holmdel, NJ, and worked on the circular electric waveguide and masers. He is presently working on the transmission aspect of a light communications system. He is the author of four books.

Dr. Marcuse is a Fellow of the Optical Society of America. He is the recipient of the 1981 Quantum Electronics Award of the IEEE, and of the 1989 Max Born Award of the Optical Society of America.